IOSR Journal of Applied Physics (IOSR-JAP)
e-ISSN: 2278-4861.Volume 8, Issue 1 Ver. I (Jan. - Feb. 2016), PP 47-56
www.iosrjournals

HVOF Sprayed WC-Cocr Coating on Mild Steel: Microstructure and Wear Evaluation

Dibyendu Naha[1], Soumen Chatterjee[2], Manojit Ghosh[1], J. Dutta Majumdar[3], Abhijit Majumdar[4†]

[1]*Department of Metallurgy and Materials Engineering, Indian Institute of Engineering Science and Technology, Shibpur, Howrah-03, W.B., India*
[2]*School of Materials Science and Engineering, IIEST, Shibpur, Howrah-03, W.B. India.*
[3]*Department of Metallurgical & Materials Engineering, IIT, Kharagpur, India-721302*
[4]*Department of Physics, Indian Institute of Engineering Science and Technology, Shibpur, Howrah-711103, W. B., India*

Abstract: *The microstructure, the wear and corrosion behavior of WC-CoCr coatings, deposited on mild steel substrate by High Velocity Oxygen-Fuel (HVOF) flame-spraying, were examined as a function of oxygen flow ratio, standoff distance and powder feed rate during the deposition process. It is observed that the surface roughness, micro hardness and fretting wear of the coated film depends on the stand off distance at a constant power feed rate. At elevated stand off distance the surface roughness increases while the micro-hardness decreases. Fretting wear study shows the applicability of the coating whereas potentio-dynamics scanning reveals the corrosion property as well as the possible galvanic coupling effects between the substrate and the coating. A crude statistical model is proposed where the process parameters have been varied using a 2^k factorial experimental design and it is constituted of two types of variables: responses (Roughness) and factors (stand off distance, fuel/oxygen ratio, powder feed rate). The statistical model is well agreed with the experimental values.*

Key words*: High velocity oxygen fuel, WC-CoCr, Fretting wear, Surface roughness, Potentio-dynamic scanning, factorial design.*

I. Introduction

Owing to their excellent wear resistance property, electrodeposited hard Cr coatings have been extensively used since many years for a wide variety of applications, including bushing pins, printing and corrugating rolls, ball valves, machine tools, fittings, hydraulic cylinders, rotating shafts, bearing journals, aircraft landing gear, pistons, undersea oilfield equipment etc.[1] However, there are crucial environmental and health issues related to the presence of hexa-valent Cr (CrVI) from chromic acid, used during the plating process. Cr-VI is known to be carcinogenic and to cause a wide array of medical problems.[2] The alternative coatings to hard Cr has to be wear resistant and at the same time offer mechanical properties of similar or better than hard Cr coating. In addition, the new coatings must be resistant to environmental corrosion. Presently, carbide-based cermets coatings deposited by HVOF spray have exhibited the best results, especially in the manufacturing and maintenance operations on military and civil aircrafts for components such as landing gears, propellers and hydraulic actuators. Deposited by HVOF thermal spray, these coatings are dense and exhibit very high adhesive strength and micro hardness. HVOF is a widely used thermal spray process by which particles are heated and propelled at very high velocities (>1 mach) resulting from the internal combustion of oxygen and fuel (propylene, kerosene, natural gas, hydrogen, etc.) inside a specially designed spray gun. In particular, WC-CoCr deposited by HVOF has been chosen as one the best candidates for landing gear components and a large number of groups worldwide have been studying it and testing this material for diverse applications.[3-11] In most of the situations it exhibit a superior wear performance than electrolytic hard Cr and better corrosion resistance.[12-13] and it does not affect the fatigue strength of the material. The coating is composed of WC particles in a matrix of CoCr. Cr is added to increase the atmospheric corrosion resistance. A great deal of effort has been recently devoted in investigating the HVOF process including the effect of microstructure of HVOF-sprayed coatings,[14-22] in-flight particle properties,[23-25] and process parameters,[24-27] on resulting wear behavior. In the above studies, a general trend has been observed about the effect of in-flight particle properties on resulting microstructure and wear resistance of the coatings; the higher the particle's velocity and temperature, the denser, more coherent and more wear resistant the coating is. In other studies, involving the effect of process parameters have considered carrier gas flow rate,[24-30] standoff distance,[24-31] powder feed rate,[29-30] and substrate surface speed [23]. These studies indicated major factors controlling the particle in-flight properties, and hence wear behaviour to be the powder feed rate and the gas flow rate, while there has been some ambiguity about the effect

of standoff distance on the in-flight particle properties and the resulting wear behavior.[32-36] This uncertainty and lack of accurate distinction of the different effect(s) of the various spraying factors may, very well, be due to their interaction effects, which have not been dealt with in the previous attempts.[23] In the light of the above, a need for a more distinguishing method of analysis is obvious, i.e. a proper methodology should be able to, quantitatively; determine the effects of the various process parameters as well as their interaction effects which sometimes could be more prominent than the effects of separate factors themselves.[31]

In this study a full factorial 2^k design of experiments (DOE) has been employed to pre-plan the experiments for further analysis of the results. Factors investigated in this study were fuel-oxygen flow ratio, standoff distance and powder feed rate during the coating process [32]. The relative influence of these parameters, either individually or combined, on the surface roughness of the coating has been evaluated using the empirical model after analysing the experimental data.

II. Experimental

Mild steel with 127 (l) x 127 (d) mm and 5 mm thickness plates were thoroughly sand blasted to enhance the binding force between the substrate and the deposited coating. Coating was deposited by HIPOJET 2700 thermal spraying system. In order to determine the individual process parameters distinctly and quantitatively, a distinguishing method of analysis is obvious, i.e. a proper methodology that should be able to determine the effects of the various process parameters as well as their interaction effects which sometimes could be more prominent than the effects of separate factors themselves.[31] Process parameters investigated for the present investigations include fuel gas (LPG) to Oxygen flow ratio, standoff distance and powder feed rate during the coating process. Two levels (high and low) were used for each factor, yielding eight different experimental combinations.

X-ray diffraction (XRD) pattern has been measured by means of Co Kα radiation. SEM pictures were taken using GEOL machine. TEM image were recorded by TECNAI, 200 kv, G2ST, FEI. Roughness of as coated samples was measured using Mitutoyo make SJ-210 surface roughness tester.

Fretting wear test has been carried out to evaluate the wear performance of the coatings. Fretting wear study has been conducted using fretting wear tester Winducom 2006-RFM.TR-285M using 10N load in order to evaluate the wear resistance performance of the coating. The high values of the process parameters includes stand off distance (A, in mm), fuel/oxygen flow ratio (B) and power feed rate (C, in rpm) are 400, 0.27 and 8.5, respectively. Similarly, the low values of these process parameters are 100, 0.23 and 6.5, respectively.

III. Theoretical Model

The aim is to optimize or model the process by performing each experiment and draw conclusions about the significant behavior of the investigated objects. The two types of variables; responses and factors constitute in this model. The responses yield information about the investigated system while the factors are used to manipulate it. During the present work "Roughness" is response and "Stand of Distance, Fuel/ Oxygen ratio, Powder feed rate" are the factors. These modifications take effect on the responses and can be measured.

Many experiments involve a study of the effects of two or more factors on the response of interest. Factorial designs are most efficient for this type of experiment. By a full factorial experiment, all possible combinations of the discrete possible values or levels of the factors can be investigated. Accordingly, with a levels of factor A, b levels of factor B and c levels of factor C, each replicate contains all a×b×c treatment combinations. Such an experiment allows studying the effect of each factor on the response variable, as well as the effects of interactions among factors on the response variable. A 2^3 full factorial experimental design with 3 factors, namely stand off distance (A), fuel/ oxygen ratio (B), powder feed rate (C), for which there are three main effects (A, B, C), three two – factor interaction effects (AB, AC, BC) and one three factor interaction effect (ABC). To estimate all these main effects and interaction affects on the response variable (roughness), 7 degrees of freedom (df) is needed along with 1 df each for each of the seven effects making at least 8 experimental trials. Therefore, a 2^3 full factorial experiment will be most efficient to handle this requirement.

In a 2^k factorial design, it is easy to express the result of the experiments in terms of a regression model, because the regression model approach is much more natural and intuitive than the other methods like means model. The fit regression model for 2^3 factorial designs is;

$$Y = \beta_0 + \beta_1 x_1 + \beta_2 x_2 + \beta_3 x_3 + \beta_{12} x_1 x_2 + \beta_{13} x_1 x_3 + \beta_{23} x_2 x_3 + \beta_{123} x_1 x_2 x_3 + \varepsilon \quad \ldots\ldots. (1)$$

Where the coded variable x_1, x_2, x_3 represents the factors A, B and C, respectively. The terms x_1x_2, x_1x_3, x_2x_3 represents AB, AC and BC interactions, respectively. The term $x_1x_2x_3$ represents the ABC interaction, and the β's regression coefficients which are estimated by half of the corresponding factor effect, that is; β_1 = (Effect of A)/2, β_2 = (Effect of B)/2, β_3 = (Effect of C)/2, β_{12} = (Interaction effect of A and B)/2, β_{13} = (Interaction effect of A and C)/2, β_{23} = (Interaction effect of B and C)/2, β_{123} = (Interaction effect of A, B and C)/2, where, β_0 is the coefficient for the intercept and ε represent the residual.

IV. Results

4.1. Surface Morphology

Mild steel plate as substrate and WC-CoCr powder as coating material has been used through HVOF coating technique in the present investigation. The coating material used in this study was commercially available Sulzer Metco made WOKA3652 having composition is about W:Co:Cr:C:Fe = 83.1: 8.5: 3.4: 4.8: 0.2 and and particle size distribution between −45 to +15 µm.

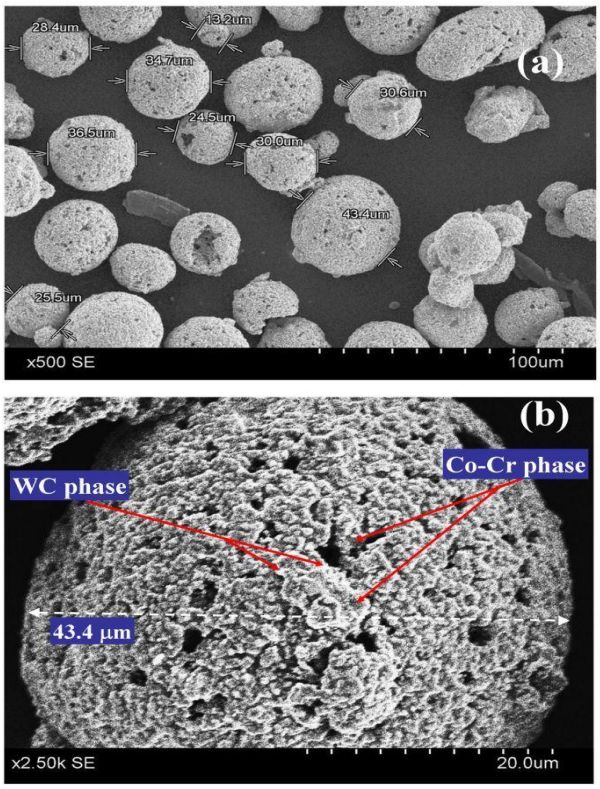

Figure 1. SEM picture of WC-CoCr (a) powders (b) a single particle

Figure 1 captures the shape of the powders using SEM technique and it is clear that, the powders have spherical agglomerated appearance. The microstructure of the powders exhibits the presence of two phases, the brighter areas are WC particles, while the dark areas are the CoCr metal matrix (fig 1b).[28] Figure 1b shows a high density of blocky angular particles of carbides, well bonded with the metallic binder phase. TEM image (inset fig. 2a) indicates that the size of the powder is not in the nanometer scale. The SAD pattern (fig 2a) also corroborates this fact. Figure 2a exhibits particle in the nano-meter range and the corresponding SAD reflects crystallographic plane (101) and (110) of WC. Figure 2b shows different peaks for elements present inside the particle. The coated surfaces were characterized in terms of microstructure, tribological and corrosion properties.

4.2. Microstructure Characterization of Coated Surface

The metallographic investigation revealed similar coating microstructure for all specimens. The cross section of coating 8 is shown in figure 3a that clearly represent dense coating with very good contact with the substrate resulting good bonding to the substrate. The representative SEM images at the cross section of the as sprayed coatings are shown in figure 3. The coating shows blocky carbide grains with somewhat rounded edges in a CoCr binder matrix. The WC particles are distributed uniformly throughout the coating. Comparing sample 6 and sample 8, where fuel oxygen ratio for sample 6 has increased keeping other parameters constant, coating 6 exhibits most densely packed structure devoid of microcracks and porosity and consequently shows highest hardness. Maintenance of high fuel-oxygen ratio, for sample 6, compared to coating 8, (two other process parameters are same) has been spotted responsible for the exhibition of denser coating. Reportedly,[24-27] increased fuel-oxygen ratio increases temperature and velocity of the in-flight particle. This is associated with increase in kinetic energy that helps in flattening the particle upon impact and provides improved adhesion to the substrate and lowers porosity in the coating.[34]

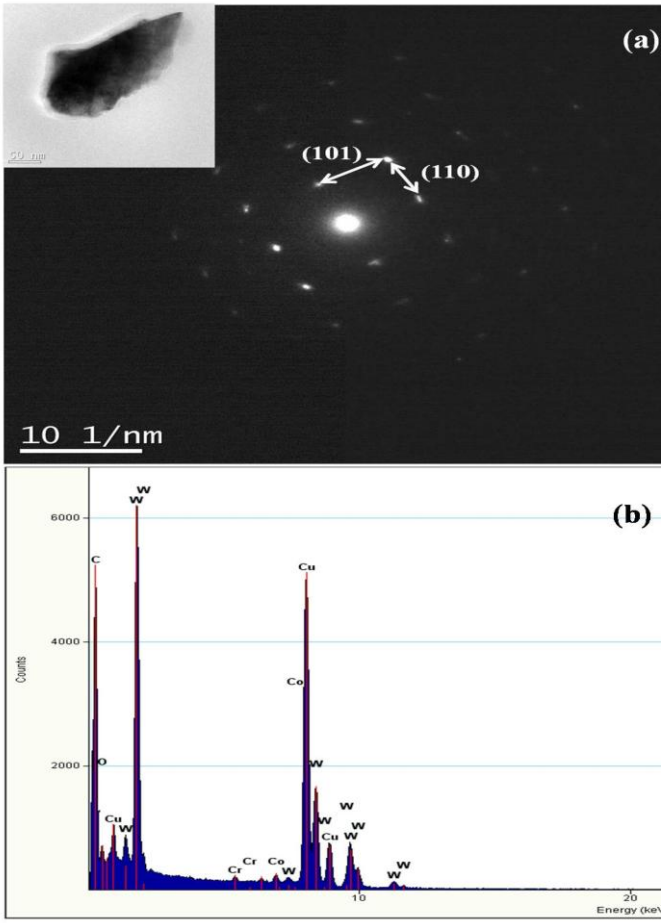

Figure 2. TEM picture of (a) a single WC-Co-Cr powder particle and SAD pattern of the corresponding particle (b) elemental analysis on the particle

The effect of standoff distance can be examined by comparing coating 7 and coating 8 where standoff distance was varied keeping two other parameters (powder feed rate and fuel-oxygen ratio) constant. Coating 7 clearly exists with large size pores and micro-cracks. Increase of standoff distance resulted with decrease of particle temperature, velocity and hence kinetic energy leading to deterioration of coating quality.[34, 35] Comparison of coating 2 with coating 6 or coating 3 with coating 7 reflects the influence of powder feed rate. Clearly high powder feed rate (applicable for coating 2 and coating 3) does not generate quality coating as coating 2 and coating 3 are full of porosity and micro cracks. With increase of powder feed rate particle temperature and velocity reduces.[24-28] As kinetic energy depends on velocity, with the decrease of velocity, kinetic energy also decreases which affects particle flattening and increase coating porosity.

Figure 4 shows the XRD patterns for the WC-Co-Cr powder and two other coating deposited by HVOF processes. WC is the major phase identified both in powder and coating and shows maximum intensity at 100 and 101 planes. Also, the intensity of all WC peaks is higher in powder compared to coated specimens. Small amount of Co and Co_3W_3C phase in as-sprayed powders are also present. Evidences of de-carburization in the coatings (to a small extent) through dissociation of WC particles to W_2C, have been observed. However, no sign of oxidation in the coating is seen. XRD (fig 4) of powder exhibits peaks corresponding mostly to WC with very small intensity peaks of Co and η phase (W_3Co_3C).

Figure 5 shows the wear depths as a function of time for different coatings. Here it can be observed wear rate is highest for mild steel substrate. As it can be observed there is very little difference in the wear rate of various coatings produced by varying process parameters, except only in case of coating sample 6. Coating 6 shows the highest wear rate as well as the highest hardness. Excessive decarburization experienced in these conditions, which was associated with rapid carbide dissolution during spraying, resulted in lowering of the wear resistance. Even though the hardness of W_2C is higher than that of WC, the presence of the more brittle

W_2C phase surrounding the WC particles, results in a decrease in wear resistance. Also, the enrichment of CoCr binder phase in W and C increases its hardness and involves the development of a more brittle binder phase.

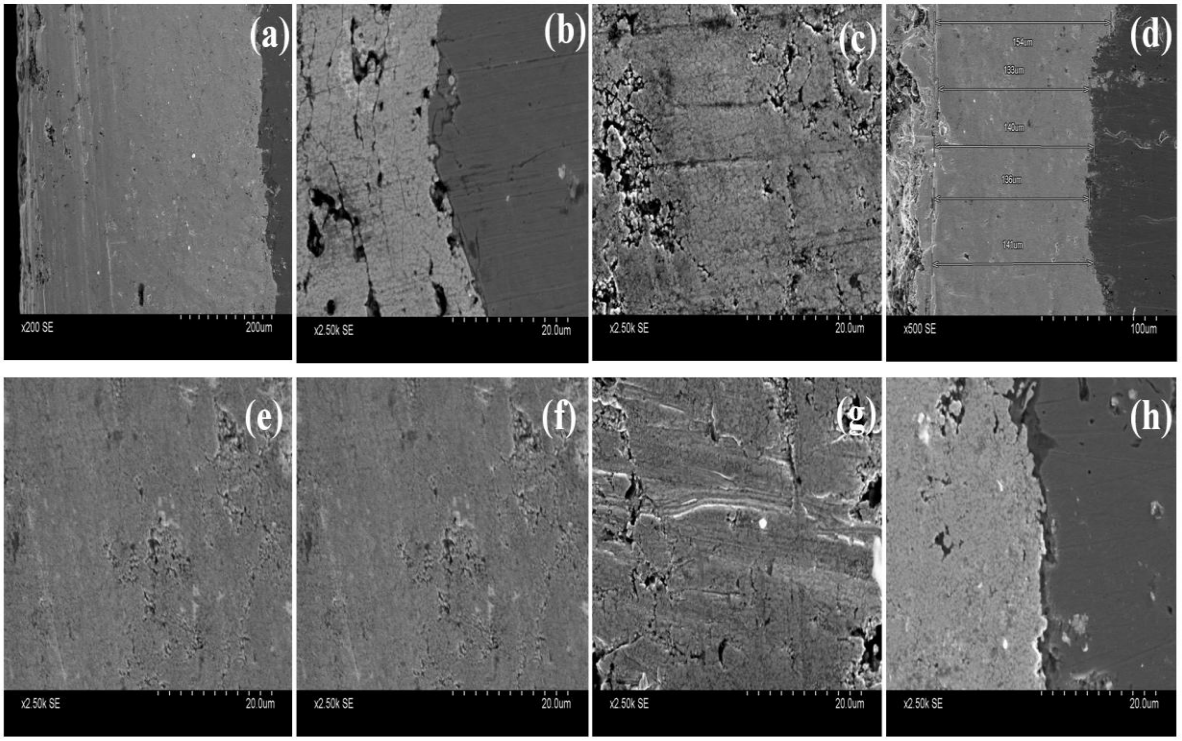

Figure 3. SEM micrograph of the cross section of HVOF spray deposited (a) Coating 2 (b) Coating 6, (c) Coating 3 and (d) Coating 7

The Micro-hardness of the coatings (Hv) has been measured on the prepared cross sections of the sprayed coating using 100 gmf load. Each result is an average of 7 measurements and the accuracy is ± 2 % for a confidence level of 0.95.

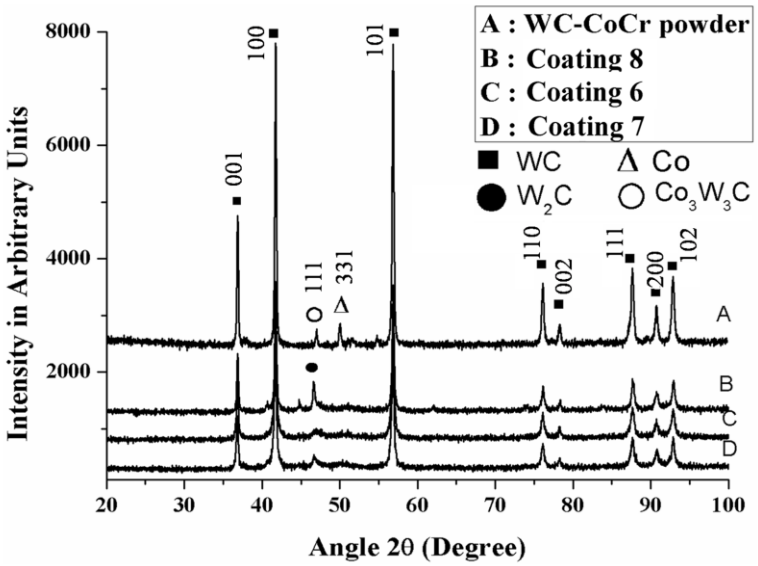

Figure 4. XRD diffraction patterns of the WC-CoCr powder and coating sprayed by the HVOF processes

Comparing results of coating 6 and 8 (fig. 3) it can be observed that, lowering fuel-oxygen ratio with powder feed rate and standoff distance constant, surface roughness increases by 24.2% for sample 8 (table 1). Appearance of less dense coating due to low fuel-oxygen ratio was found responsible for this. Increase of

surface roughness by 22.7% in one case (comparing coating 3 and coating 4) and almost similar values for another situation (coating 7 and coating 8) is exhibited during increment of standoff distance. Sensitivity of surface roughness is therefore more with higher powder feed rate (45.33 gm/mm) operations compared to the one (34.66 gm/mm) applied for coating 7 and coating 8. However, larger surface roughness with higher standoff distance commensurate with the reason stated earlier.[34] The influence of powder feed rate can be investigated by comparing coating 3 with coating 7 and coating 2 with coating 6 for two different values of standoff distance (400 and 100 mm respectively). With higher powder feed rate (45.33 gm/min) and larger constant standoff distance (400 mm) increase of surface roughness is recorded (comparing coating 2 and coating 6). This is corroborated to the fact that coating porosity decreases with increase of in-flight velocity and temperature, which is resulted from decrease in powder feed rate. The combined effect of high velocity and temperature attribute to the deformation of agglomerate on impact, so that the solidifying splats will be able to conform to the surface of the previously deposited layer and fill the pores and defects.[35] Although, for higher powder feed rate (45.33 gm/min) and smaller constant standoff distance (100 mm), hardly any noticeable change in surface roughness values are observed (comparing coating 3 and coating 7).

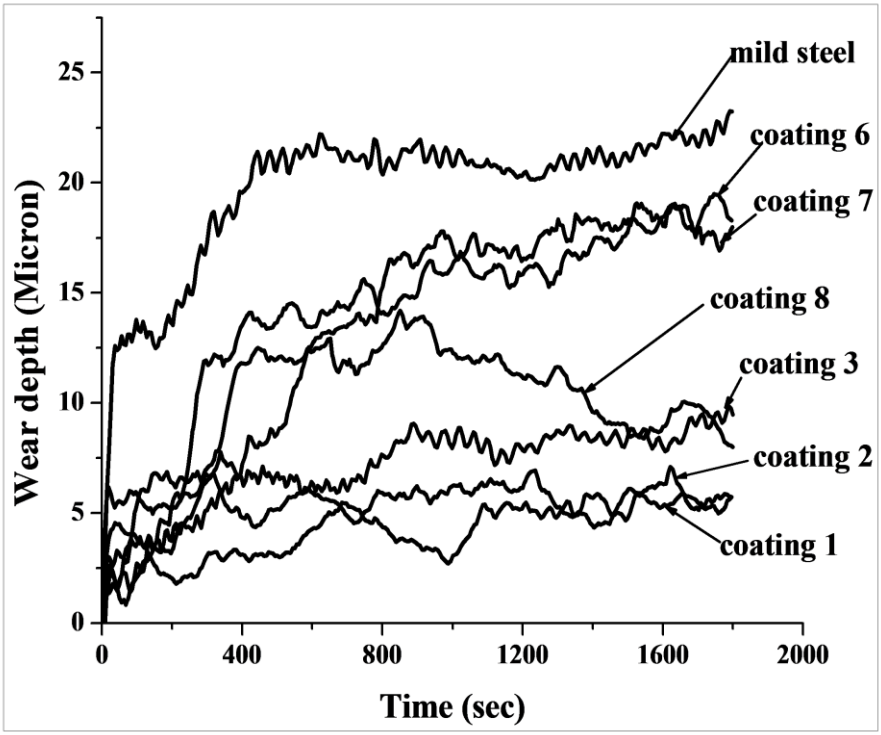

Figure 5. Wear depth Vs time plot for coated and uncoated specimens

The comparative picture of micro-hardness data of the coating undergoing different processing conditions are shown in table 1. The micro-hardness of the coatings varies between 1020 and 1594 Hv. The variations of micro-hardness values among different HVOF coatings are significant. Coating 6 has highest hardness where as coating 4 have lowest hardness. In general coating hardness increases with increasing the particle temperature and particle velocity.[24]

Potentio dynamic scanning studies on coated and uncoated samples have been conducted using a potentiostat of AutoLab. A conventional three - electrode cell set up consisting of the working electrode, a saturated calomel electrode as the reference electrode and a platinum counter electrode was used. All tests were carried out in 3.56 wt% sodium chloride (NaCl) solution at room temperature (23 ºC). Samples were scanned in the range -0.44 to + 1.0 Volt in order to obtain full anodic and cathodic polarization curves. Potentiodynamic scanning generates corrosion potential (E_{corr}), corrosion current (I_{corr}) and corrosion rate for all coated and uncoated samples shown in table 2. All coating exhibited much higher corrosion rate as compared with uncoated mild steel substrate which justifies the purpose of the work. Further, all coated and uncoated sample displayed negative E_{corr} values. Higher I_{corr} values of the coated samples when compare with the mild steel substrate from the Potentiodynamic scanning studies reveals high degree of porosity / presence of voids and micro-cracks within the coating. It is likely that the coatings contain numerous networks of continuous voids, pores and cracks that extend from the coating surface through to the substrate. Such findings are in agreement with previously studies.[36-37]

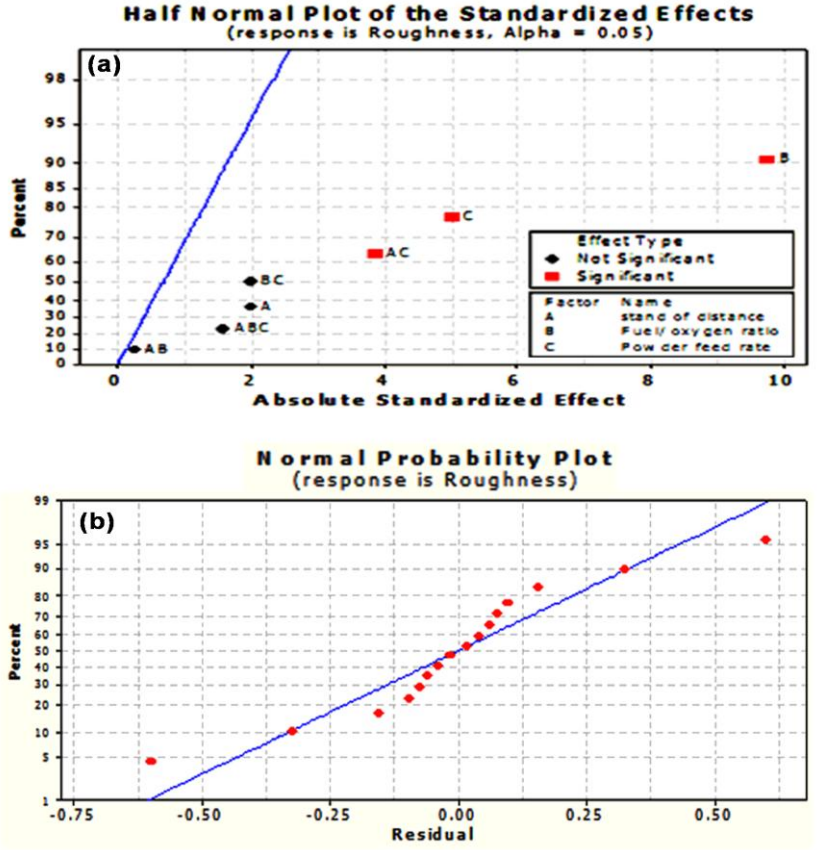

Figure 6. (a) The half normal probability plot of the effect estimates for the above experiments. This is a plot of the absolute value of the effect estimated with respect to their cumulative normal probabilities and (b) a normal probability plot of the residuals.

V. Discussion

Statistical analysis of the measured roughness data, represented in table 3, was carried out using DOX software. In the theoretical estimation we put alternative low and high values to cross check the roughness values. Each sample was replicated for five times to minimize the error in surface roughness data tabulated in table 3. The resulting error range has also been presented in the same table. Table 4 summarizes effect estimates, sum of squares and percent contribution of the factors. This results indicate that the largest effects on roughness are from fuel/oxygen ratio (B = -1.7412), powder feed rate (C = -0.8938) and the stand off distance-powder feed rate interaction (AC = -0.6862). Table 5 may be used to explain through ANOVA that other two effects e.g. A & BC also have some amount of significance on roughness. These experiments were analyzed, (figure 6) and a statistical model has been developed. Figure 6(a) shows the half normal probability plot of the effect estimates for the above experiments. This is a plot of the absolute value of the effect estimated against their cumulative normal probabilities. Many analysts felt that the half-normal plot is easier to interpret, particularly when there are only a few effect estimates (8 in this case) conforming to this work.[19]

Figure 6(a) also shows that the important effects that emerged from this analysis (indicated by their large distance from the straight line depicted in figure 6(a)) are the fuel/oxygen ratio (B), powder feed rate (C), and the interaction between stand of distance and powder feed rate (AC). The stand off distance however, does not have the same level of effect compared to other two individual factors. The fuel/oxygen ratio has been the dominant factor followed by powder feed rate and interactions effect between standoff distance and powder feed rate. In figure 6(a), it can also be noticed that BC interaction has more effect on the roughness than the stand of distance factor alone, indicating the fact that interaction effects could exceed the effects of some principal process parameters.

In figure 3, SEM image of coating 1 (a) and coating 3 (c) has been presented. In these coatings fuel-oxygen flow ratio has been varied keeping other process parameters constant. Coating 3 has higher fuel-oxygen ratio compared to coating 1.

Comparing figures it can be concluded coating 1 has more porous structure compare to coating 3, indicating increasing fuel-oxygen ratio helps to form better coating structure with improved roughness. Also observing coating 1 and coating 5 (e) in figure 3, where powder feed rate has varied keeping other parameters constant. It can be inferred that coating 5 is less porous in comparison to coating1; indicating coating 5 is less rough compared to coating 1.

In this model (2) we get the roughness is estimated given below:
Roughness= 7.819375 + 0.1769A-0.8706B–0.4469C +0.3431 AC -0.1769 BC. (2)

Residual analysis is performed to check the adequacy of the model (2). The model is tested against normality of its residuals. A normal probability plot of the residuals is shown in figure 6(b). The points on this plot lay reasonably close to a straight line, lending support to the fact that A, B, C, AC and BC extend significant effects. The experiments were performed randomly, and in order to check the independent assumptions, plotting the residual vs fitted value of the data was performed as shown in figure 6(b). A tendency to have runs of positive and negative residuals indicates positive correlation. Figure 7(a), however shows no correlation between residuals.

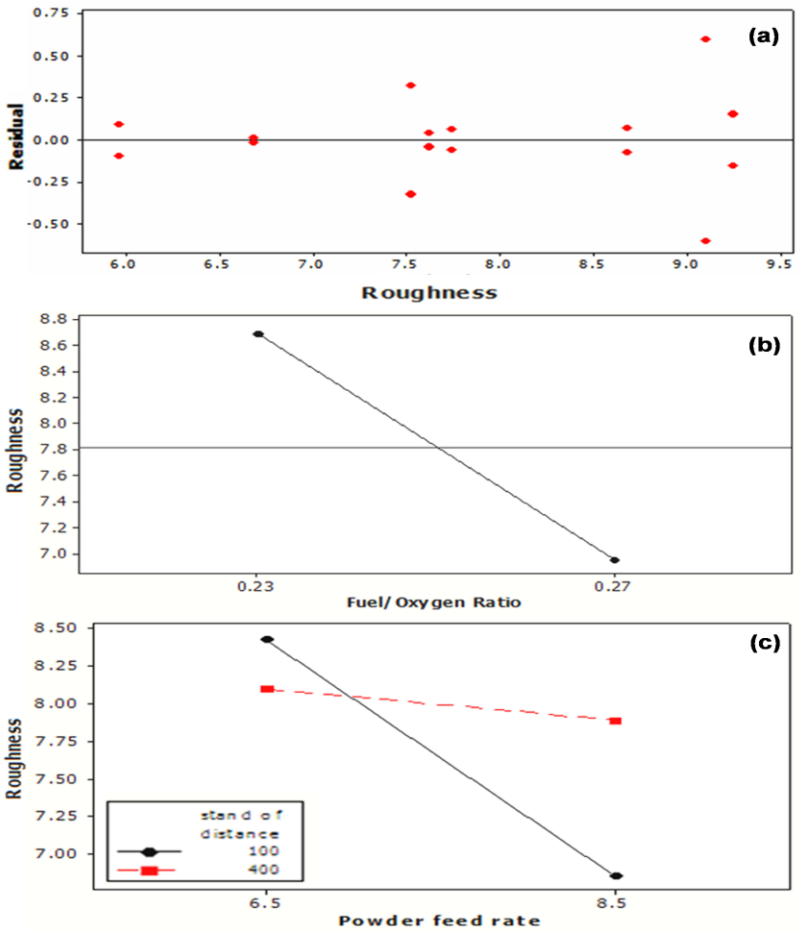

Figure 7. (a) Estimated/fitted value of roughness with respect to (a) residual, (b) fuel/oxygen ratio and (c) powder feed rate.

The analysis of variance (ANOVA) in table 5 was used to confirm the magnitude of these effects. As noted from table 5, the main effects of fuel/oxygen ratio (B) and powder feed rate (C) are highly significant(both have very small p value, 0.00 and 0.004 respectively).The main effect is evident in figure 7(b) and figure 7(c), where greater roughness are favored by a low powder feed rate and low fuel/oxygen ratio. The AC interaction is also highly significant; thus there is a strong interaction between stand off distance and powder feed rate. As mentioned above, the two-factor-interaction effect between the stand off distance and powder feed rate (AC) had more prominent effect than the stand off distance factor alone. This interaction effect is evident in Figure 7(c), where greater roughness values are favored by a high powder feed rate and a high stand off distance.

VI. Conclusions

Higher fuel/oxygen ratio, lower powder feed rate and shorter standoff distance shows better mechanical properties with less pores and micro-cracks in the coated structure. Hardness of coating increases with increasing fuel/oxygen ratio. Surface roughness increases with increasing standoff distance, however the degree of increase is related with the powder feed rate. At present experimental conditions, fuel-oxygen ratio shows more influence than the powder feed rate and that has higher influence than the spray distance. Fretting wear study of selected samples shows maximum wear for mild steel substrate which justifies the applicability of the coating. Potentio dynamic scanning, on the other hand reveals poor corrosion performance of the WC-CoCr coatings compared to mild steel substrate. This may be attributed to poor structure and possible galvanic coupling effects between the substrate and the coating.

Acknowledgements

Authors thanks to Mr. Shantanu Newar, Director, Eastern Metallizing Co. Pvt. Ltd (EMCL) to perform HVOF coating treatment at EMCL is acknowledged. The assistance by Dr. Malay Kundu during the SEM investigation is also gratefully acknowledged. Authors would like to acknowledge the resourceful academic discussion with late Professor N. Bandyopadhyay, Tata steel chair professor, Indian Institute of Engineering Science and Technology Shibpur,, West Bengal, India.

References

[1]. K.R. Newby, Industrial (Hard) Chromium Plating, Surface Engineering, ASM Handbook, ASM International, Materials Park, OH, 1994, pp. 177-191.
[2]. H. J. Gibb, P. S. J. Lees, P. F. Pinsky, B. C. Rooney, 2000 Am. J. Ind. Med. **38** 15-126.
[3]. K. O. Legg, Overview of Chromium and Cadmium Alternative Technologies, Surface Modification Technologies XV, T.S.Sudarshan and M. Jeandin, Ed., ASM International, Materials Park, OH, 2002, pp. 1-10.
[4]. P. M. Natishan, S. H. Lawrence, R. L. Foster, J. Lewis, B. D. Sartwell, 2000 Surf. & Coat. Tech. **130** 218-223.
[5]. J. A. Picas, A. Forn, G. Matthaus, 2006 Wear **261** 477-484.
[6]. L. Thakur, N. Arora, R. Jayaganthan, R. Sood, 2011 Appl. Surf. Sci. **258** 1225– 1234
[7]. H. Wang, X. Wang, X. Song, X. Liu, X. Liu, 2015 Appl. Surf. Sci. **355** 453–460.
[8]. J. A. Picas, Y. Xiong, M. Punset, L. Ajdelsztajn, A. Forn, J. M. Schoenung, 2009 Int. J. of Refractory Metals & Hard Materials **27** 344–349.
[9]. S. H. Zhang, T. Y. Cho, J. H. Yoon, W. F., K. O. Song, M. X. Li, Y. K. Joo, C. G. Lee, 2008 Materials Characterization **59** 1412-1418.
[10]. C. Reigner, A. Sturgeon, D. Lee, D. De Wet, HVOF Sprayed WC-Co-Cr as a Generic Coating Type for Replacement of Hard Chromium Plating, Proceedings of the International Thermal Spray Conference, May 2002 (Dusseldorf, Germany), 2002, pp. 12-16.
[11]. D. Dudzinski, P. Au, J.G. Legoux, S. Simard, Salt Fog Corrosion Resistance of HVOF WC-10C0-4Cr Coated and Electrolytic Hard Chromium Plated AerMet 100 and 300M Steel Alloys, Proceedings of the International Thermal Spray Conference, May 2002 (Dusseldorf, Germany), 2002, pp. 686-692.
[12]. D. Lee, E. Eybel, R. Evans, Development and Implementation of HVOF WC-CoCr Coating as Alternative to Electrolytic Hard Chrome Plate in Landing Gear Applications Using Natural Gas as Fuel, Thermal Spray 2003,Orlando, FL, 2003, pp. 371-376.
[13]. B. Sartwell, K. O. Legg, J. Schell, J. Sauer, P. Natishan, D. Dull, J. Falkowski, P. Bretz, J. Deveraux, C. Edwards, D. Parker, Validation of HVOF WC/Co Thermal Spray Coatings as a Replacement for Hard Chrome Plating on Aircraft Landing, An open report from Naval Research Laboratory, code No. 6170, 2004, pp. 209-214
[14]. A. Lekatou, E. Regoutas, A.E. Karantzalis, 2008 Corrosion Science **50** 3389–3400.
[15]. H. Liao, B. Normand, C. Coddet, 2000 Surf. & Coat. Tech. **124** 235–242.
[16]. Josep A. Picas, Elisa Rupérez, Miquel Punset, Antonio Forn, 2013 Surf. & Coat. Tech. **225** 47–57.
[17]. G. Marginean, D. Utu, 2010 Surf. & Coat. Tech **205** 1985–1989.
[18]. J.A. Picas, M. Punset, M. T. Baile, E. Martín, A. Forn, 2011 Surf. & Coat. Tech **205** S364–S368.
[19]. E. Fleury, S. M. Lee, J. S. Kim, D. H. Kim, W. T. Kim, H. S. Ahn, 2002 Wear **253** 1057-1069.
[20]. H. Liao, B. Normand, C. Coddet, 2000 Surf. & Coat Tech. **124** 235-242.
[21]. Q. Yang, T. Senda, A. Ohmori, 2003 Wear **254** 23-34.
[22]. J. Wang, K. Li, D. Shu, X. He, B. Sun, Q. Guo, M. Nishio, H. Ogawa, 2004 Mat. Sci. Eng. A **371** 187-192.
[23]. W. Lih, S. Yang, C. Su, S. Huang, I. Hsu, M. Leu, 2000 Surf. & Coat. Tech. **133** 54-60.
[24]. L. Zhao, M. Maurer, F. Fischer, R. Dicks, E. Lugscheider, 2004 Wear **257** 41-46.
[25]. A. Ghabchi, S. Sampath, K. Holmberg, T. Varis, 2014 Wear **313** 97–105.
[26]. L. Thakur, N. Arora, 2013 Wear **303** 405–411.
[27]. G. Bolelli, L. Lusvarghi, M. Barletta, 2009 Wear **267** 944–953.
[28]. J. A. Picas, A. Forn, G. Matthaus, 2006 Wear **261** 477–484.
[29]. T. Zhang, D.T. Gawne, Y. Bao, 1997 Surf. & Coat. Tech. **96** 337-334.
[30]. J. C. Tan, L. Loonney, M. S. J. Hashmi, 1999 J. Mat. Proc. Tech. **92** 203-208.
[31]. D. C. Montgomery, Design and analysis of experiments, Sixth ed., John Wiley and Sons, New York, 2005.
[32]. J. A. Picas, M. Punset, M. T. Baile, E. Martın, A. Forn, 2009 Plasma Process. Polym. **6** S948–S953.

[33]. D. Srinivas Rao, D. Sen, K. R. C. Somaraju, S. Ravi Kumar, N. Ravi, G. Sundararajan, The influence of powder particle velocity and temperature on the properties of Cr_3C_2–25NiCr coating obtained by detonation gun, in: Proceedings of the 15th International Thermal Spray Conference, Nice, France, 1998, pp. 385–394.
[34]. B. R. Marple, J. Voyer, J. F. Bisson, C. Moreau, 2001 J. Mat. Proc. Tech. **117** 418-423.
[35]. J. E. Cho, S. Y. Hwang, K. Y. Kim, 2006 Surf. & Coat. Tech. **200** 2653-2662.
[36]. E. Celik, I. Ozdemir, E. Avci, Y. Tsunekawa, 2005 Surf. & Coat. Tech. **193** 297-302.